

T/L-Shaped Zeroth-Order Resonators Loaded Microstrip Antenna with Enhanced Bandwidth for Wireless Applications

Kai Sun¹, Lin Peng^{1, 2, *}, Quan Li¹, and Xing Jiang¹

Abstract—New zeroth-order resonators (ZORs) are utilized as parasitic elements to enhance a microstrip antenna's bandwidth. By utilizing mushroom T/L shaped resonators, extra resonances are generated. Then, by merging the resonances of the microstrip antenna and the T/L shaped resonators, a wideband antenna is obtained to cover the 5.15–5.35 GHz wireless local area network (WLAN) band. As the ZORs are embedded in the patch of the microstrip antenna, the usages of the parasitic elements do not increase the antenna size. Moreover, as one ZOR resonance is lower than the microstrip patch resonance, a compact antenna is realized. The patch size is decreased from $0.27\lambda_c \times 0.42\lambda_c \times 0.027\lambda_c$ of the reference microstrip antenna (RMA) to $0.25\lambda_c \times 0.40\lambda_c \times 0.026\lambda_c$ of the proposed ZOR based microstrip antenna, where λ_c is the wavelength of their corresponding lower cutoff frequencies. The proposed antenna was fabricated and measured. The simulated and measured -10 dB impedance bands of the proposed antenna are 5.06–5.40 GHz and 5.07–5.42 GHz, respectively. And, its bandwidth increases 70% compared to the RMA. The simulated and measured patterns are stable in the whole operating band. The gains of 4.73 dBi and 4.24 dBi are measured at the ZOR modes, and 7.88 dBi is measured at the microstrip patch mode.

1. INTRODUCTION

With the rapid development of wireless communication technology, many systems need miniaturized and broadband antennas. The U.S. Federal Communications Commission (FCC) announced the allocation of three 100 MHz bands in the 5 GHz band for the use as a U-NII (unlicensed national information infrastructure) band to provide fast turn-on and high-speed wireless data communications. Three 100 MHz frequency bands are 5.15 ~ 5.25 GHz for the provisions of its EIRP not more than 23 dBm and suitable for indoor wireless communications, 5.25 ~ 5.35 GHz band that provides EIRP not more than 30 dBm for short-range communications, and 5.725 ~ 5.825 GHz band that provides EIRP not more than 36 dBm for medium distance communication. The traditional microstrip antennas were widely used because of their many advantages, such as low profile, light weight, low cost, and easy construction [1]. However, the narrow impedance bandwidth (such as 2%) of a microstrip antenna has become a major restriction for practical application [2]. In order to overcome this shortcoming, bandwidth broadening microstrip antenna technologies have been studied. Parasitical patches were utilized to generate multi-resonances with a bandwidth 12.6%, but the antenna size is large [3]. The technique of decreasing Q value by low permittivity (air gap), thick substrate and capacitive feeding is used for bandwidth enhancement [4, 5]; however, the antenna's profile is high. In [6], a butter fly shape patch increases the bandwidth from 11.41% to 21.50%. Though wideband can be obtained by the multi-layer structure and fold structure technologies the antenna profile and complexity are greatly increased [7, 8]. In [9], a microstrip antenna is allied with rectangular waveguide for a 70% bandwidth, but the antenna is bulky.

Received 3 November 2017, Accepted 10 January 2018, Scheduled 19 January 2018

* Corresponding author: Lin Peng (penglin528@hotmail.com).

¹ The Guangxi Key Laboratory of Wireless Wideband Communication and Signal Processing, Guilin University of Electronic Technology, Guilin, Guangxi 541004, China. ² Guangxi Experiment Center of Information Science, Guilin, Guangxi 541004, China.

Zeroth-order resonators (ZORs) are very small, and they are suitable for antenna applications. A novel ZOR structure loaded circular microstrip patch was proposed in [10]. The antenna had a monopole antenna radiation performance and effectively reduced the antenna cross-section and size. In [11], new zeroth-order resonators (ZORs) were utilized as parasitic elements to enhance the bandwidth of a microstrip antenna, and the measured impedance bandwidth is increased from 56 MHz of the reference microstrip antenna to 133 MHz of the ZORs loaded antennas. However, the parasitic elements lead to antenna size enlargement. In [12], a wideband folded mushroom zeroth-order resonance (ZOR) antenna combines the TM_{010} ($\lambda/2$) mode and ZOR mode to obtain a wide bandwidth of 68%; however, due to the folding structure, the structure of the antenna is very complicated. In [13], a hybrid zeroth-order resonance (ZOR) patch antenna also combined a TM_{010} ($\lambda/2$) mode and a ZOR mode with a bandwidth of 3.3% while the E -plane HPBW of the proposed antenna was measured as 115° and broadened by 53%, compared with that of the conventional rectangular patch antenna. In [14], the antenna was loaded by ZOR and complementary split-ring resonator (CSSR) units, and the antenna resonated at three frequency bands. Similarly, in [15], the zeroth-order and TM_{10} modes of a composite right/left-handed (CRLH) mushroom resonator were investigated with regard to the number of cells. The structure also demonstrated multi-resonances.

In this research, the bandwidth of a microstrip antenna is enhanced by embedding T/L-shaped mushroom ZORs in the patch of an RMA. By merging the resonances of the ZORs and the microstrip patch modes the bandwidth of the proposed antenna is increased by 70%, from the microstrip antenna's 200 MHz to the proposed antenna's 340 MHz. As the ZOR structures are placed in the interior of the microstrip patch, the antenna size is unchanged with decreasing frequency, and the microstrip patch mode still has good performances.

2. ANTENNA DESIGN

The proposed antenna fed by a coaxial probe is shown in Figure 1. It can be seen that the antenna consists of two parts. One part is the traditional rectangular microstrip patch, and the other is T/L-

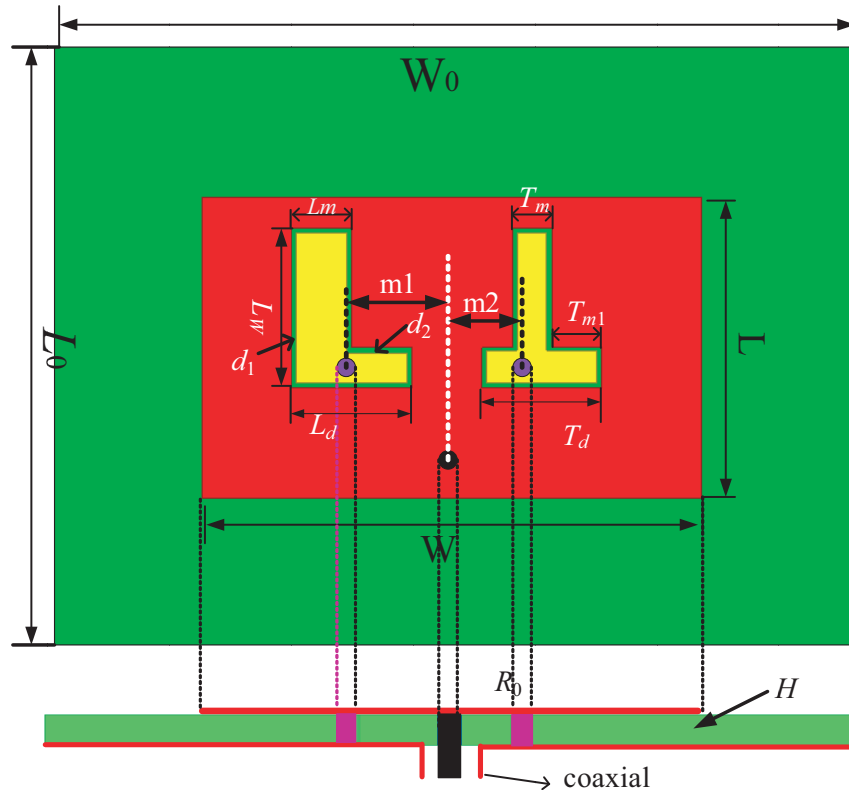


Figure 1. Configurations of the antenna.

shaped mushroom ZORs embedded in the patch. The two ZORs have different structures (T and L) and resonances, then, by merging the resonances of the RMA and the T/L-shaped ZORs, the antenna's bandwidth can be enhanced. As the ZOR structures are very small, their embedding has little impact on the field distributions of the microstrip patch mode. Thus, the microstrip patch mode maintains good radiating performances. The antenna was fabricated on an F4b-2 substrate (in green) with a relative dielectric constant of 2.65, thickness of 1.6 mm, and tangential loss of 0.002. Parameters of the antennas are as follows: $W = 40$ mm, $L = 30$ mm, $W = 25$ mm, $L = 15$ mm, $L_w = 7.5$ mm, $L_d = 6$ mm, $L_m = 3$ mm, $m_1 = 4.9$ mm, $m_2 = 3.5$ mm, $T_d = 5.5$ mm, $T_m = 2$ mm, $Tm_1 = 2.5$ mm, $R = 0.5$ mm, $d_1 = 0.25$ mm, $d_2 = 0.5$ mm, $d_3 = 0.25$ mm.

The design methodology is to generate new resonant modes in a microstrip antenna and merge them with the microstrip patch mode to form a broadband. The new resonators should be small, then, they can be embedded in the microstrip patch to keep the compact size. Meanwhile, the small resonators have little impact on the field distribution of the microstrip patch mode to maintain good radiating performances of the microstrip patch mode. For these purposes, the very compact T/L-shaped ZORs are chosen. Then, to further clearly show the mechanism of the design method, four antennas, the RMA, an antenna with L-shaped ZOR, an antenna with *T-shaped* ZOR and the proposed T/L shaped ZOR antenna, are investigated for comparison as shown in Figures 2(a) and (b). As expected in Figure 2(c), it can be clearly seen that the RMA, L-shaped ZOR antenna, *T-shaped* ZOR antenna and T/L-shaped ZOR have one, two, two and three resonance points, respectively. Different numbers of resonance points appear, and the main reason is that each resonance point is generated by a certain part (resonator) of the antenna. For example, a conventional microstrip patch antenna generates a resonant point at 5.3 GHz. When the *L-shape* or *T-shape* patch is added to the antenna, the antenna generates new resonances at 5.2 GHz or 5.35 GHz. While adding both the *L-shape* and *T-shape* structures to the microstrip patch, the antenna does add two more resonance points. Compared to the RMA, L-shaped ZOR antenna and

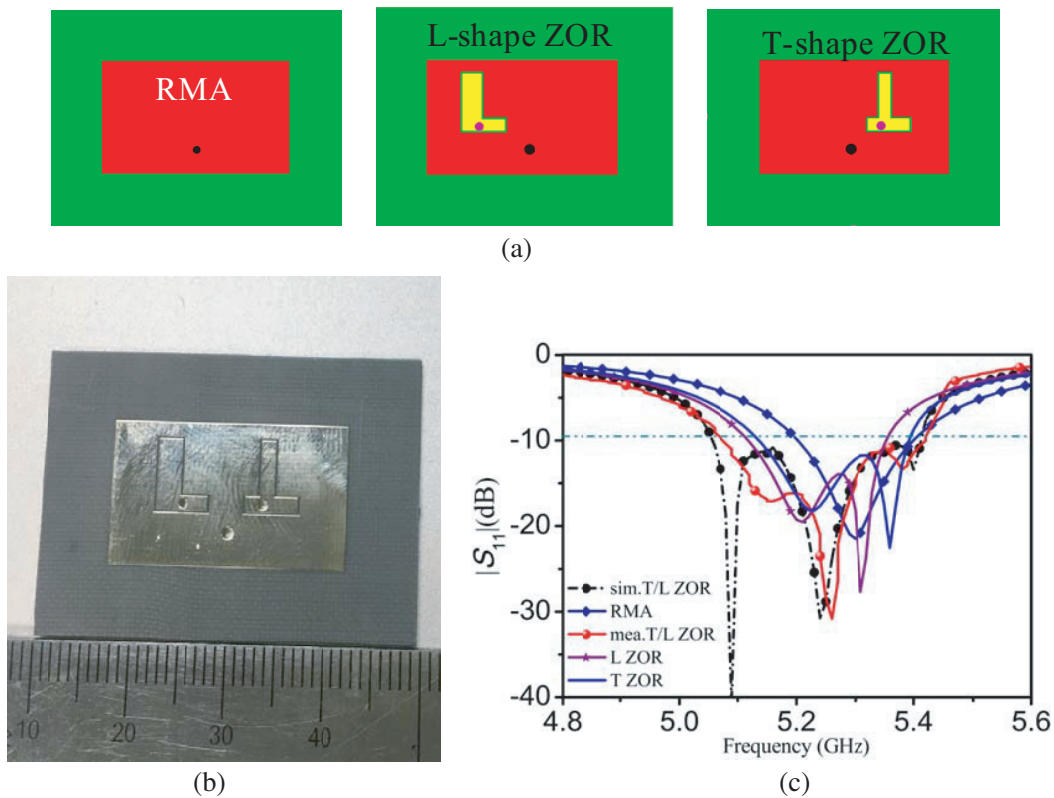


Figure 2. The structures and reflection coefficient of the antennas. (a) The structures of the RMA, the L-shape ZOR, the T-shape ZOR. (b) The photography of the antenna. (c) Simulated and measured reflection coefficient of antennas.

T-shaped ZOR antenna, the bandwidth of the proposed antenna is increased by 140 MHz (about 70%) and 70 MHz (about 27%, including the *L-shape* and *T-shape* antennas), respectively. The measured -10 dB impedance band of the T/L-shaped ZOR antenna is from 5.07 GHz to 5.42 GHz, and it fully covers the WLAN frequency from 5.15 GHz to 5.35 GHz. Though, small discrepancies are observed between the simulated and measured results, reasonable agreement is also obtained.

3. ANTENNA ANALYSES AND DISCUSSION

The material dispersion affects the propagation characteristics of the electromagnetic wave, and the material in nature has a positive dielectric constant and permeability [16], while the metamaterials are dispersive, and their constitutive parameters can be zero or negative. As a class of metamaterials, the ZOR's constitutive parameters reflect its characteristics. To verify the ZOR features of the embedded resonators, the constitutive parameters of the resonators are retrieved by the Kramers-Kronig relationship based metamaterial parameters extraction method [17]. As demonstrated in Figure 3(a), microstrip line based models are built to imitate the operational environment of the ZOR as in the microstrip antenna. The *L-shape* ZOR and *L-shape* ZOR models are established. The microstrip line uses the same substrate as the designed antennas. Figure 3(b) exhibits the constitutive parameters curves of L-ZOR and T-ZOR. As shown in the figure, resonances occur for both the L-ZOR and T-ZOR as large mutations happen for the effective permittivity (ϵ_{reff}) and effective permeability (μ_{reff}) curves. For both L-ZOR and T-ZOR, as can be seen from the frequency-electrical parameter curve, the permittivity and permeability change with frequency. In particular, the dielectric constant shows a negative value near the resonance point, and their μ_{reff} s are close to zero at the frequencies. Then, it can be judged that the embedded structures are ZOR resonators.

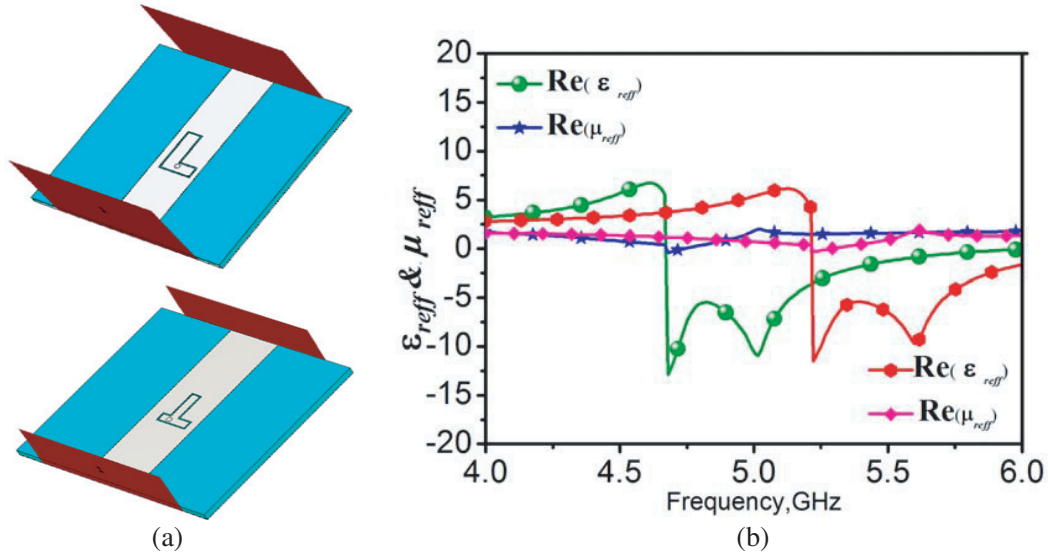


Figure 3. (a) The microstrip equivalent model. (b) Dielectric constant and permeability.

As the three resonant modes of the proposed ZOR-based antenna correspond to different resonators, it is supposed that the *L-shaped* ZOR, microstrip patch and *T-shaped* ZOR dominate the three simulated matching pole frequencies independently. Current distributions indicate the operational mechanism of an antenna. Then, to reveal the characteristics of the proposed ZOR-based antenna, current distributions of the three resonances $f = 5.10$ GHz, $f_1 = 5.25$ GHz and $f_2 = 5.39$ GHz of the antenna are plotted in Figures 4(a), (b) and (c), respectively. As shown in Figure 4(a), the currents of $f = 5.10$ GHz are mainly concentrated in the L-shaped ZOR. From Figure 4(b), the currents of $f_1 = 5.25$ GHz are focused at the microstrip patch especially at the left and right edges of the patch. In Figure 4(c), the currents of $f_2 = 5.39$ GHz are concentrated in the T-shaped ZOR. Then, it can be expected that the

resonance frequencies can be adjusted by the parameters of their corresponding resonators. Though the currents of f , f_1 and f_2 mainly distribute at their corresponding resonators as also demonstrated in Figures 4(a), (b) and (c), there are still some currents spread to other resonators, meaning that modes couplings happen for the proposed antenna [18, 19]. For the T-ZOR/L-ZOR/microstrip patch, they can be equivalent to RLC resonators [20] as described in Figure 4(d). Most of the dissipated power (represented by the resistance R) of the resonators radiates to the space. However, some of the power is in the form of surface wave and travels on the patch surface, then, power interchanging (modes couplings) between the resonators happens as described in Figure 4. The modes couplings will cripple the independency of the resonators.

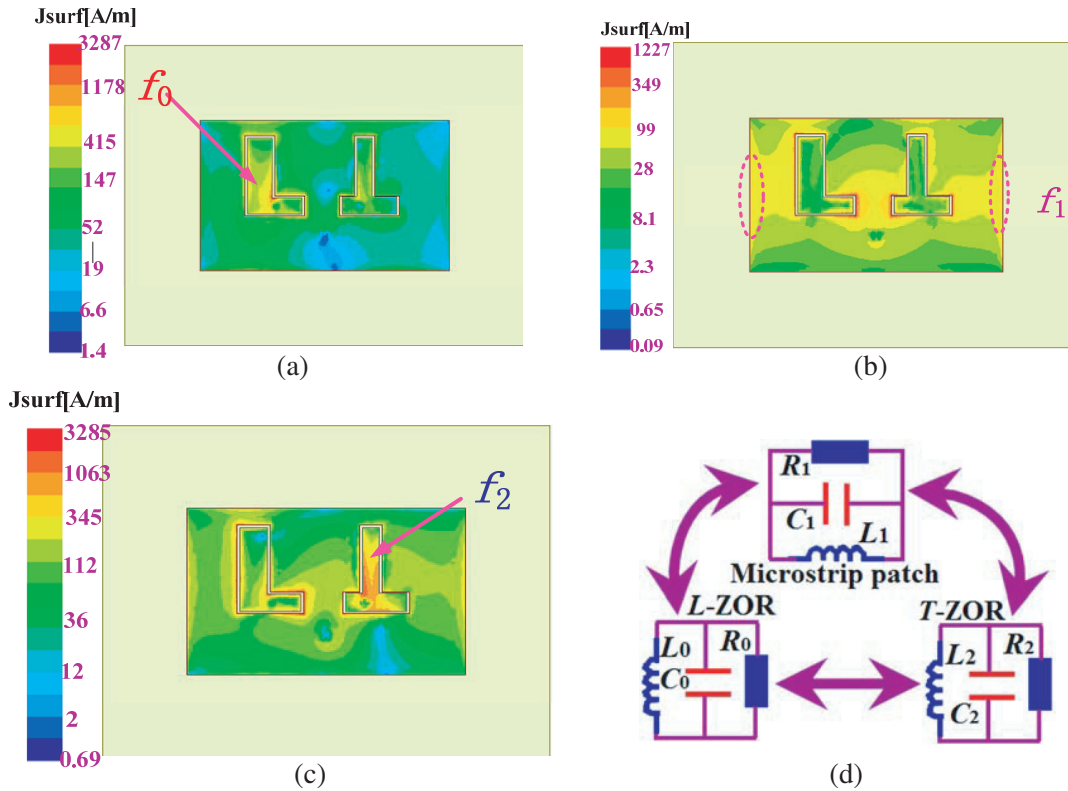


Figure 4. Current distributions of T/L ZOR antenna. (a) $f_0 = 5.1$ GHz, (b) $f_1 = 5.25$ GHz, (c) $f_2 = 5.39$ GHz, and (d) antenna coupling model.

The impedance curves of the RMA and the proposed ZOR-based antenna are shown in Figure 5. It is clear from Figure 5(a) that the RMA has a resonance point that leads to good impedance matching around 5.3 GHz. From Figure 5(b), L -shaped and T -shaped ZORs loaded structure resonates at three frequencies. Each resonance corresponds to one resonator. As half-wavelength resonator, the RMA mode has smaller Q factor value. Then, its impedance curves are more smooth, while the electrically small ZORs are strong resonant structures, and they have larger Q factor values. Then, their impedance curves appear relatively cliffy.

To further reveal the characteristics of the resonant modes, parametric studies are conducted as shown in Figure 6 and Figure 7. Figure 6 presents the results for the parameters m_1 and m_2 . Note that the changes of m_1 and m_2 only move the vias. As shown in Figure 6(a), by increasing of parameters m_1 from 4.8 mm to 5.0 mm with a step of 0.1 mm, the resonance frequency f_0 increases from 5.06 GHz to 5.10 GHz and 5.15 GHz, while f_1 and f_2 are little impacted. Similarly, from Figure 6(b), the resonance f_2 increases from 5.34 GHz to 5.36 GHz and 5.39 GHz by increasing m_2 from 3.3 to 3.4 and 3.5 mm, while the other resonances are little moved.

The parametric studies on L_d and T_d are shown in Figure 7. As L_d and T_d are related to the sizes

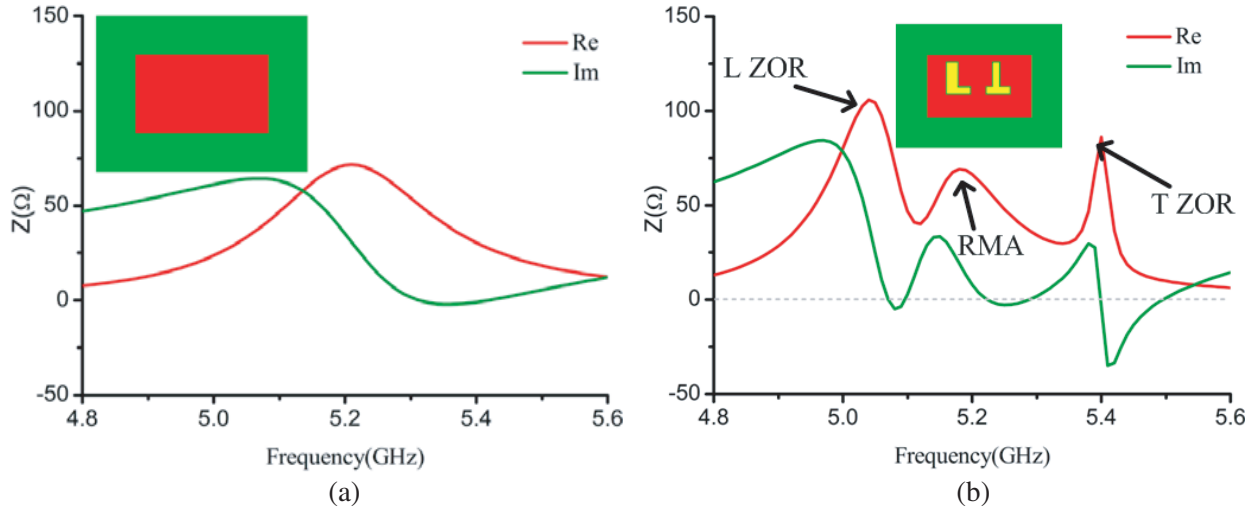


Figure 5. The impedance curves of the antennas. (a) RMA, (b) the proposed ZOR based antenna.

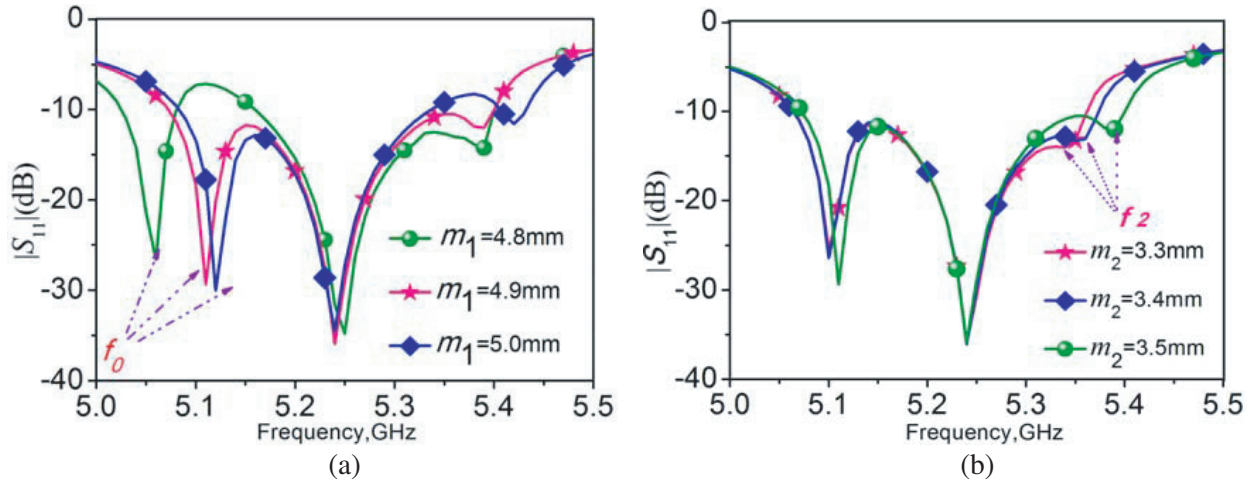


Figure 6. Parameter sweep for T/L ZOR antenna. (a) m_1 , (b) m_2 .

of the *L-shape* ZOR and *T-shape* ZOR, respectively, it is expected that the corresponding resonant frequency will be changed by adjusting the parameters. As shown in Figure 7(a), by reducing the parameters L_d from 6 mm to 5.4 mm with a step of 0.3 mm, the resonance frequency f_0 is increased from 5.06 GHz to 5.12 GHz and 5.15 GHz, while only very small impact happens to f_1 and f_2 . Similarly, from Figure 7(b), the resonance f_2 is increased from 5.39 GHz to 5.44 GHz and 5.49 GHz by reducing the T_d from 5.5 to 5.2 and 4.9 mm, while the other resonances are almost unchanged.

The results in Figure 6 and Figure 7 confirm the independency of the resonators. Then, the three resonant frequencies of the proposed ZOR-based antenna can be tuned by adjusting their corresponding parameters. Though tuning one resonant mode would have some impacts on the other resonant modes owing to modes couplings discussed in Figure 4, these impacts are very small, and the resonant frequencies can still be tuned with little effect on the other.

The radiation patterns of the proposed T/L ZOR antenna are measured by the NSI2000 system in a microwave anechoic chamber as shown in Figure 8(a). The simulated and measured radiation patterns of the three matching pole frequencies $f_0 = 5.15$ GHz, $f_1 = 5.25$ GHz, and $f_2 = 5.39$ GHz are exhibited in Figures 8(b), (c) and (d), respectively. It can be seen from the figures, all the microstrip patch mode and ZOR modes radiate unidirectionally. It is clear that the measured results agree well with the

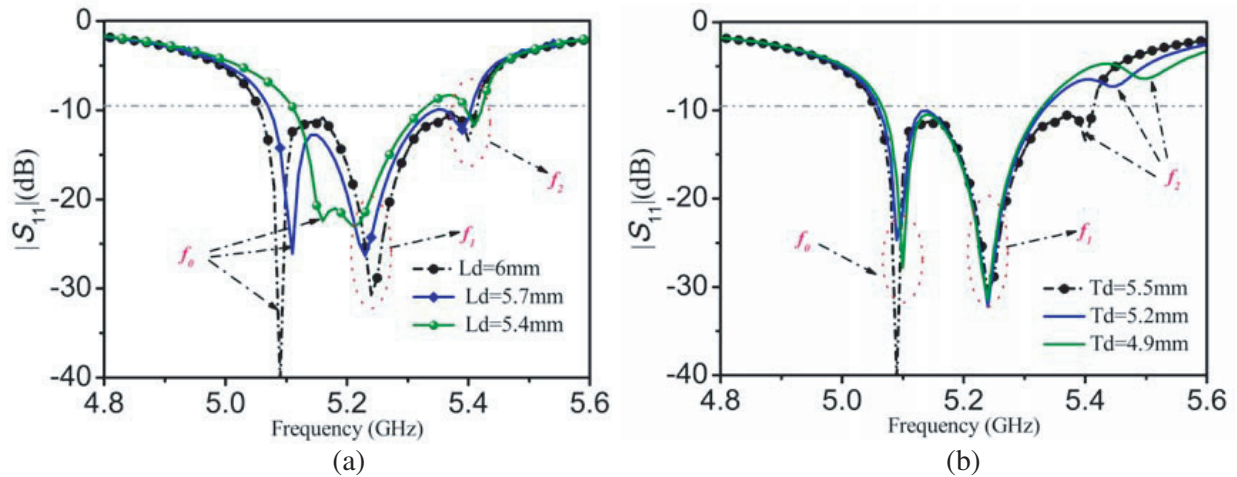
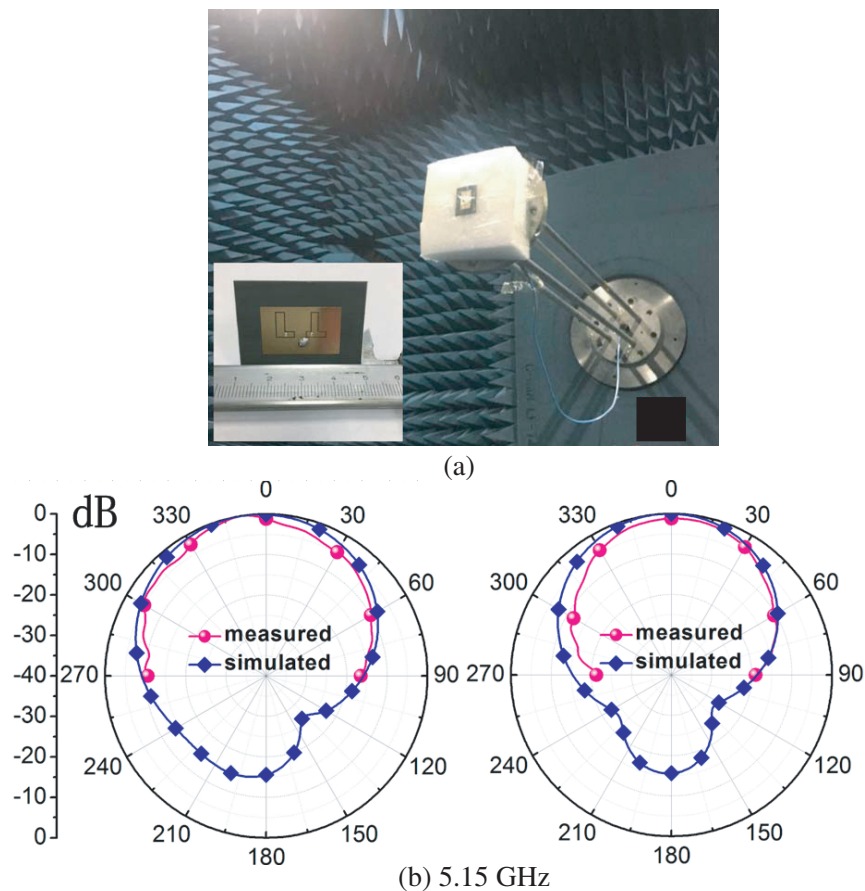


Figure 7. Parameter sweep for T/L ZOR antenna. (a) L_d , (b) T_d .

simulated ones. Note that only half space is measured as the backed platform of the measuring system rejects back radiation measuring.

The simulated and measured gains of the proposed T/L-ZOR based antenna are demonstrated in Figure 9. The measured gains of the ZOR modes of the proposed T/L-ZOR based antenna are 4.73 dBi and 4.24 dBi for f_0 and f_2 , respectively, while the gain of the microstrip patch mode (f_1) is 7.88 dBi. It is found that the gains of the ZOR frequencies are smaller than the microstrip patch mode. It is



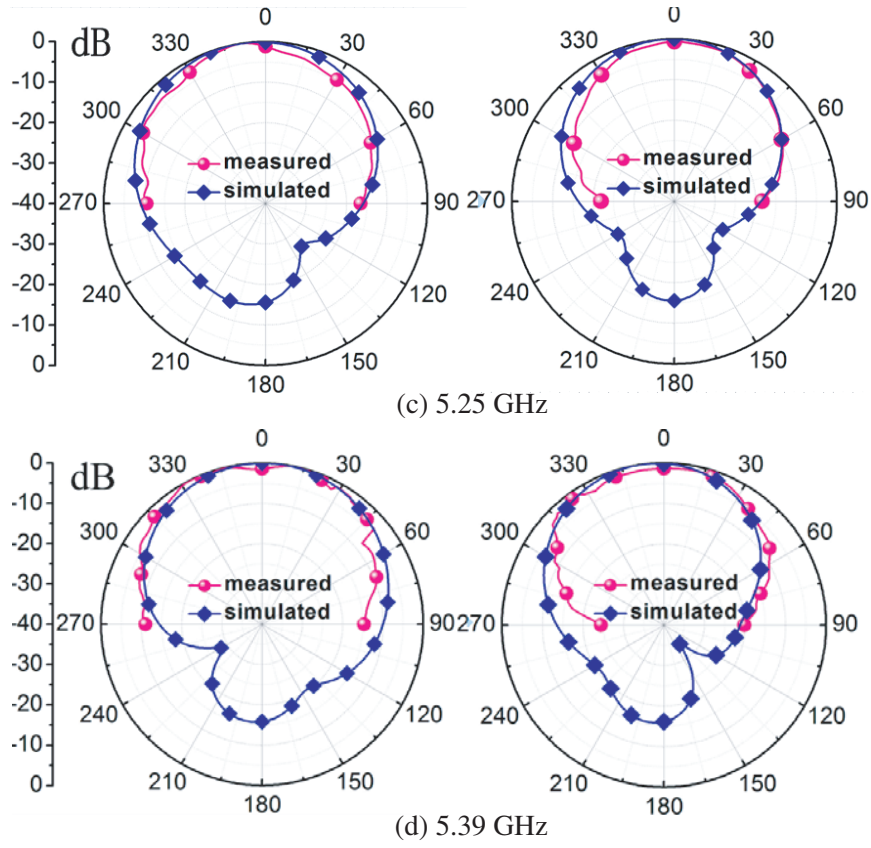


Figure 8. Radiation patterns of T/L ZOR antenna. (a) The environment of measurement, (b) f_0 , (c) f_1 , and (d) f_2 .

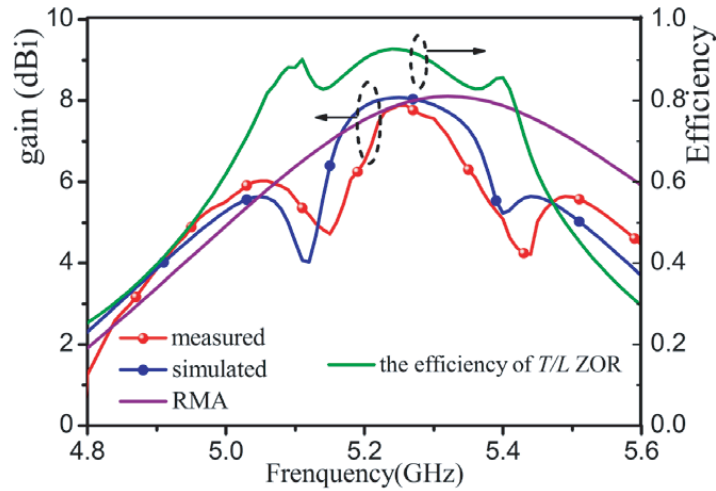


Figure 9. Gain and efficiency of T/L ZOR antenna.

because the sizes of the *L-shape* and *T-shape* ZORs are electrically small ((microstrip antenna size $0.25\lambda_c \times 0.40\lambda_c$, L-shape ZOR size $0.13\lambda_c \times 0.10\lambda_c$, T-shape ZOR size $0.13\lambda_c \times 0.098\lambda_c$)), then, their gains are small as antenna gain is related to the antenna size. At the microstrip patch mode, its gain is comparable with the RMA. The efficiency curve of the proposed antenna is also demonstrated in Figure 9. The antenna efficiency of the proposed antenna is not bad in the band, such as 93%, though

the efficiencies drops a little near the ZOR modes. At the ZOR frequencies (f_0 and f_2) of the antenna, the antenna's radiation efficiencies are 83% and 80%, respectively. Though the gains of the ZOR modes are smaller than the microstrip patch mode, they still obtain moderate values. Moreover, the embedded ZORs maintain compact size of a microstrip antenna while enhancing the impedance bandwidth. Thus, the proposed antenna is useful for wireless applications.

4. CONCLUSION

In this paper, a wideband T/L-shaped ZOR microstrip antenna is proposed. The T/L-shaped ZORs are embedded in the microstrip antenna, then, the merging of the microstrip patch mode and ZOR modes leads to bandwidth enhancement. The bandwidth of the proposed antenna increases 70% compared to the RMA. The corresponding impedance bandwidth is 5.06–5.40 GHz, covering the 5.15–5.35 GHz wireless local area network (WLAN) band. Good radiation patterns and gain curves are also obtained. The characteristics and operational mechanism of the proposed antenna are discussed. The design method can be easily applied to other frequency bands.

ACKNOWLEDGMENT

This work was supported in part by the National Natural Science Foundation of China under Grant Nos. 61401110 & 61661011 & 61371056, in part by Natural Science Foundation of Guangxi under Grant No. 2015GXNSFBA139244, and in part by Innovation Project of GUET Graduate Education under Grant No. 2016YJXC76 & 2017YJXC30.

REFERENCES

1. Sabban, A., "New wideband printed antennas for medical applications," *IEEE Trans. Antennas Propag.*, Vol. 61, No. 1, 84–91, 2013.
2. Mandal, K. and P. P. Sarka, "High gain wide-band U-shaped patch antennas with modified ground planes," *IEEE Trans. Antennas Propag.*, Vol. 61, No. 4, 2279–2282, 2013.
3. Cao, W. Q. and W. Hong, "Bandwidth and gain enhancement for probe-fed CP microstrip antenna by loading with parasitical patches," *Progress In Electromagnetics Research Letters*, Vol. 61, 47–53, 2016.
4. Verma, A. K. and Nasimuddin, "Resonance frequency of rectangular microstrip antenna on thick substrate," *Electronics Letters*, Vol. 37, 1373–1374, 2001.
5. Peng, L., C. L. Ruan, and X. H. Wu, "Design and operation of dual/triple-band asymmetric M-shaped microstrip patch antennas," *IEEE Antennas Wireless Propag. Lett.*, Vol. 9, 1069–1072, 2010.
6. Tiwari, R. N., P. Singh, and B. K. Kanaujia, "Butter fly shape compact microstrip antenna for wideband applications," *Progress In Electromagnetics Research Letters*, Vol. 69, 45–50, 2017.
7. Peng, L., J. Y. Xie, and S. M. Li, "Wideband microstrip antenna loaded by elliptical rings," *Journal of Electromagnetic Waves and Applications*, Vol. 30, No. 2, 154–166, 2016.
8. Guha, D., C. Sarkar, and S. Dey, "Wideband high gain antenna realized from simple unloaded single patch," *IEEE Trans. Antennas Propag.*, Vol. 63, No. 10, 4562–4566, 2015.
9. Shetti, N. M., "Waveguide coupled microstrip patch antenna a new approach for broad band antenna," *Progress In Electromagnetics Research C*, Vol. 72, 73–79, 2017.
10. Yoo, S. and S. Kahng, "CRLH zor antenna of a circular microstrip patch capacitively coupled to a circular shorted ring," *Progress In Electromagnetics Research C*, Vol. 25, 15–26, 2012.
11. Peng, L., J. Y. Mao, X. F. Li, X. Jiang, and C. L. Ruan, "Bandwidth of microstrip antenna loaded by parasitic zeroth-order resonators" *Microwave and Optical Technology Letters*, Vol. 59, No. 5, 2017.
12. Ko, S. T. and J. H. Lee, "Wideband folded mushroom zeroth-order resonance antenna," *IET Microwaves Antennas & Propagation*, Vol. 7, No. 2, 9–84, 2013.

13. Ko, S.-T. and J.-H. Lee, "Hybrid zeroth-order resonance patch antenna with broad-plane beamwidth," *IEEE Trans. Antennas Propag.*, Vol. 61, 19–25, 2013.
14. Mehdipour, A., T. A. Denidni, and A.-R. Sebak, "Multi-band miniaturized antenna loaded by ZOR and CSRR metamaterial structures with monopolar radiation pattern," *IEEE Trans. Antennas Propag.*, Vol. 62, No. 2, 555–563, 2013.
15. Amani, N. and A. Jafargholi, "Zeroth-order and TM modes in one-unit cell CRLH mushroom resonator," *IEEE Antennas Wireless Propag. Lett.*, Vol. 14, 1396–1399, 2015.
16. Udagedara, I., M. Premaratne, I. D. Rukhlenko, H. T. Hattori, and G. P. Agrawal, "Unified perfectly matched layer for finite-difference time-domain modeling of dispersive optical materials," *Optics Express*, Vol. 17, No. 23, 21179–90, 2009.
17. Szabo, Z., G. H. Park, R. Hedge, and E. P. Li, "A unique extraction of metamaterial parameters based on Kramers-Kronig relationship," *IEEE Transactions on Microwave Theory and Techniques*, Vol. 58, 2646–2653, 2010.
18. Schneider, V. M. and H. T. Hattori, "High-tolerance power splitting in symmetric triple-mode evolution couplers," *IEEE Journal of Quantum Electronics*, Vol. 36, No. 8, 923–930, 2000.
19. Kapon, E., J. Katz, and A. Yariv, "Supermode analysis of phase-locked arrays of semiconductor lasers," *Optics Letters*, Vol. 9, No. 4, 125–127, 1984.
20. Peng, L., J. Y. Xie, X. Jiang, and C. L. Ruan, "Design and analysis of a new ZOR antenna with wide half power beam width (HPBW) characteristic," *Frequenz*, Vol. 71, No. 1–2, 41–50, 2017.